Published in:
Advances in Cryogenic Engineering, vol. 51,
American Institute of Physics, 2006, pp. 1919-1928.

REGENERATOR OPERATION AT VERY HIGH FREQUENCIES FOR MICROCRYOCOOLERS*

Ray Radebaugh and Agnes O'Gallagher

National Institute of Standards and Technology
Boulder, CO, 80305, USA

ABSTRACT

The size of Stirling and Stirling-type pulse tube cryocoolers is dominated by the size of the pressure oscillator. Such cryocoolers typically operate at frequencies up to about 60 Hz for cold-end temperatures above about 60 K. Higher operating frequencies would allow the size and mass of the pressure oscillator to be reduced for a given power input. However, simply increasing the operating frequency leads to large losses in the regenerator. The simple analytical equations derived here show how the right combination of frequency and pressure, along with optimized regenerator geometry, can lead to successful regenerator operation at frequencies up to 1 kHz. Efficient regenerator operation at such high frequencies is possible only with pressures of about 5 to 8 MPa and with very small hydraulic diameters and lengths. Other geometrical parameters must also be optimized for such conditions. The analytical equations are used to provide guidance to the right combination of parameters. We give example numerical calculations with REGEN3.2 in the paper for 60 Hz, 400 Hz, and 1000 Hz operation of optimized screen regenerators and show that the coefficient of performance at 400 Hz and 1000 Hz is about 78 % and 68 %, respectively, of that for 60 Hz when an average pressure of 7 MPa is used with the higher frequency, compared with 2.5 MPa for 60 Hz operation. The 1000 Hz coefficient of performance for parallel tubes is about the same as that of the screen geometry at 60 Hz. The compressor and cold-end swept volumes are reduced by a factor of 47 at 1000 Hz, compared with the 60 Hz case for the same input acoustic power, which can enable the development of microcryocoolers for MEMS applications.

KEYWORDS: Cryocoolers, cryogenics, high frequency, MEMS, miniature, numerical analysis, pulse tubes, refrigeration, regenerators, Stirling.
PACS: 07.20.Mc; 43.35.Ud

INTRODUCTION

The size and mass of Stirling and Stirling-type pulse tube refrigerators are dominated by the size and mass of the pressure oscillator (compressor). The acoustic or PV power delivered by the pressure oscillator is given by

$$\dot{W}_{PV} = \tfrac{1}{2} P_1 \dot{V}_1 \cos\theta, \tag{1}$$

where P_1 and $\dot{V}_1$ are the amplitudes of the sinusoidal pressure and the volume flow, as given by

$$P = P_0 + P_1 \cos\omega t \tag{2}$$

and

$$\dot{V} = \dot{V}_1 \cos(\omega t + \theta). \tag{3}$$

The term P_0 is the average pressure, ω is the angular frequency, and θ is the phase by which the volume flow leads the pressure. The sign convention used here is that the volume flow is positive for flow out from the pressure oscillator. The volume flow amplitude is related to the instantaneous volume amplitude V_1 in the pressure oscillator by

$$\dot{V}_1 = 2\pi f V_1. \tag{4}$$

The PV power is then given by

$$\dot{W}_{PV} = \pi f V_1 P_0 \left(\frac{P_1}{P_0} \right) \cos\theta, \tag{5}$$

where f is the frequency. The term in parentheses is the relative pressure amplitude. From this equation we see that by increasing the frequency the volume amplitude V_1 can be reduced for the same PV power. An increase in the average pressure also allows for a decrease in the volume amplitude. The total swept volume of the pressure oscillator is $V_{co} = 2V_1$. Similarly the swept volume of the displacer at the cold end of a Stirling cryocooler or the volume of the pulse tube in a pulse tube cryocooler can be decreased for the same gross refrigeration power (net refrigeration plus losses) by increasing the frequency or the average pressure.

The total volume of a compressor or pressure oscillator is much larger than that of the swept volume, but there will be some correlation between the two. The total volume is typically about 100 times the swept volume, at least for 60 Hz compressors. The total compressor volume is usually proportional to the volume of the linear motor. We discuss some scaling laws for the linear motor in a later section. We recognize that the reduction factor for the entire compressor may not be as great as that of the swept volume, but a significant reduction of the compressor would be possible with higher operating frequencies. Such reductions would be very useful for space applications and for cooling of MEMS devices with micro cryocoolers built right on the same chip.

REGENERATOR FREQUENCY EFFECTS

Figure 1 shows a phasor representation for mass conservation within the regenerator of a Stirling cryocooler, where the pressure at the cold end is along the real axis. Because of the gas volume in the regenerator, the conservation of mass requires that the flow at the warm end will lead the flow at the cold end and is given by

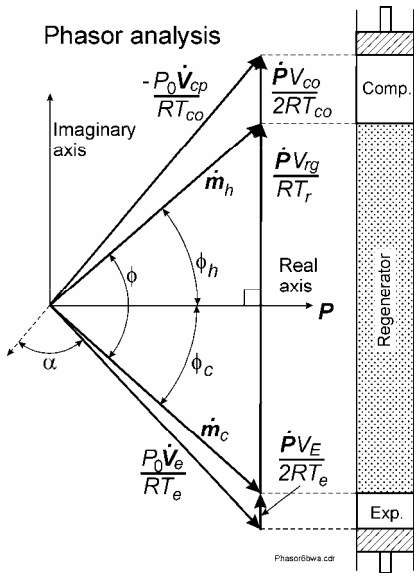

FIGURE 1. Phasor diagram representing conservation of mass inside the regenerator of a Stirling cryocooler.

$$\dot{\boldsymbol{m}}_{\boldsymbol{h}} = \dot{\boldsymbol{m}}_{\boldsymbol{c}} + \frac{\dot{\boldsymbol{P}} V_{rg}}{RT_r}, \tag{6}$$

where the bold variables represent time varying or phasor quantities, $\dot{\boldsymbol{m}}_{\boldsymbol{c}}$ is the flow rate at the cold end, V_{rg} is the gas volume in the regenerator, R is the gas constant per unit mass, T_r is the mean temperature of the regenerator, and $\dot{\boldsymbol{P}}$ is the rate of change of pressure in the regenerator, given by

$$\dot{\boldsymbol{P}} = i2\pi f \boldsymbol{P}, \tag{7}$$

where i is the imaginary unit and $\boldsymbol{P}$ is the dynamic pressure. This phasor leads the pressure by 90°, as indicated by the vertical phasor along the imaginary axis.

The optimum phase relationship between flow and pressure is that in which the flow at the regenerator midpoint is in phase with the pressure. With such a phase relationship the magnitude of flow at each end is minimized for a given acoustic power flow through the regenerator [1]. Losses in the regenerator are usually proportional to the flow magnitude. Typically the flow at the cold end will lag the pressure by about 30°, whereas at the warm end the flow will lead the pressure by about 30°. Such a phase relationship is easily achieved in a Stirling refrigerator by selecting the appropriate swept volume and phase for the displacer. The same phasor diagram would apply to a pulse tube cryocooler where the phase of the flow at the cold end would be established by an inertance tube at the warm end of the pulse tube.

According to equation (7) $\dot{\boldsymbol{P}}$ and the vertical phasor in Figure 1 increase with frequency. Thus, at very high frequencies the magnitude of the flow and the swept volume at the warm end become very large for a fixed flow at the cold end. In that case the regenerator loss becomes very high. To keep the vertical phasor from increasing significantly as frequency is increased the regenerator gas volume V_{rg} must be reduced as frequency increases. Our goal is to keep the phase angle ϕ_h nearly constant as the frequency increases. That goal is satisfied if the ratio of the vertical phasor to the mass flow amplitude is held constant as frequency is increased, *i.e.*,

$$\frac{\dot{P}V_{rg}}{\dot{m}_1 RT_r} = \frac{2\pi f P_1 V_{rg}}{\dot{m}_1 RT_r} = \text{constant}. \tag{8}$$

As the regenerator gas volume is decreased the heat transfer area must be maintained, which requires the hydraulic diameter to be reduced. Other geometrical parameters must also be changed in a manner such that the conduction loss and the pressure drop are kept constant as the volume is decreased. The next section presents an analytical expression for the ratio in equation (8) in terms of the three losses (heat transfer, conduction, and pressure drop). Such an expression will show what should be changed to keep equation (8) constant while keeping the losses constant.

REGENERATOR ANALYTICAL MODEL

The analytical model to be discussed here was first described in 1985 [2]. It was refined recently and used to show how regenerators could be made to operate at frequencies of 1 kHz or more [3]. The model may be reasonably accurate for temperatures above about 70 K. The results are summarized here. For an ideal gas the optimum gas cross-sectional area per unit mass flow rate is given by

$$\frac{A_g}{\dot{m}_1} = \left[\frac{c_p T_0 N_{Pr}^{2/3} (T_h - T_c)}{\alpha T_c P_0^2 (P_1 / P_0)^2 \cos\phi_c (\Delta P_1 / P_1)(\dot{Q}_{reg} / \dot{Q}_r)} \right]^{1/2}, \tag{9}$$

where c_p is the specific heat of the helium working fluid, T_0 is the average regenerator temperature, N_{Pr} is the Prandlt number, T_h is the hot-end temperature, T_c is the cold-end temperature, ϕ_c is the phase between the pressure and flow at the cold end, ΔP_1 is the amplitude of the pressure drop, $(\dot{Q}_{reg} / \dot{Q}_r)$ is the ratio of the regenerator thermal loss to the gross refrigeration power, and α is a dimensionless number that represents the ratio of heat transfer to pressure drop, as given by the Reynolds analogy

$$\alpha = \frac{N_{St} N_{Pr}^{2/3}}{f_r}, \tag{10}$$

where N_{St} is the Stanton number and f_r is the Fanning friction factor. The term α is a weak function of the Reynolds number and is a function of the geometry, such as screens ($\alpha = 0.05$) or parallel tubes ($\alpha = 0.31$) [3]. The optimum length and hydraulic diameter are given by

$$L = \frac{2(A_g / \dot{m}_1)(1 - n_g) \int k_{eff}\, dT}{n_g R T_c (P_1 / P_0) \cos\phi_c (\dot{Q}_{cond} / \dot{Q}_r)} \tag{11}$$

$$D_h = \left[\frac{4 b \mu T_0 (1 - n_g) \int k_{eff}\, dT}{n_g T_c P_0^2 (P_1 / P_0)^2 \cos\phi_c (\Delta P_1 / P_1)(\dot{Q}_{cond} / \dot{Q}_r)} \right]^{1/2}, \tag{12}$$

where n_g is the porosity, k_{eff} is the effective thermal conductivity of the matrix, $(\dot{Q}_{cond} / \dot{Q}_r)$ is the ratio of the conduction heat loss to the gross refrigeration power, b is the Poiseulle number, which is the product of the friction factor and the Reynolds number, and μ is the viscosity at

the average temperature. The gas volume is found by combining equations (9) and (11). Equation (8) can then be written as

$$\frac{\dot{P}V_{rg}}{\dot{m}_1 RT_r} = \frac{4\pi f N_{\mathrm{Pr}}^{2/3} c_p (T_h - T_c)(1-n_g)\int k_{eff}\, dT}{\alpha n_g R^2 T_c^2 P_0 (P_1/P_0)^2 \cos^2\phi_c (\Delta P_1/P_1)(\dot{Q}_{reg}/\dot{Q}_r)(\dot{Q}_{cond}/\dot{Q}_r)} = \text{constant.} \quad (13)$$

The last three terms in the parentheses in the denominator represent the losses in the regenerator. Typically the pressure and regenerator losses are about 20 to 25 % and the conduction loss is about 5 to 10 % of the gross refrigeration power. These losses will tend to increase some at higher frequencies to keep the ratio in equation (13) nearly constant. Note that an increase in P_0 or P_1/P_0 can compensate for an increase in f to help maintain a constant ratio in equation (13). We shall examine the case of increasing P_0 as we increase the frequency from 60 Hz to 400 Hz and then to 1000 Hz. The analytical equations (9), (11), (12), and (13) are useful for initial optimization studies, but the final optimization was carried out by way of a numerical model.

NUMERICAL ANALYSIS

Numerical Model

The NIST numerical model known as REGEN3.2, which is based on finite difference equations for the conservation equations, was used for the calculations discussed here. This model is an upgrade of REGEN3.1, described previously [4,5]. There are no changes in the numerical procedure for solving the equations except for the addition of optional boundary conditions. In REGEN3.2 we can specify the mass flow at the cold end and its phase with respect to the pressure at the cold end along with the desired average pressure and pressure ratio, and the program automatically finds the solution to meet these conditions. The mass flow at the warm end (both magnitude and phase) is calculated by the model. Losses associated with regenerator ineffectiveness, conduction through the matrix, and pressure drop are calculated by the model. Conduction loss through the tube containing the screen matrix is calculated separately. For the parallel tube geometry no separate tube loss was calculated. A loss associated with the expansion process (pulse tube or Stirling) was taken to be 20 % of the gross refrigeration power in all the cases studied. The resulting coefficient of performance (ratio of net refrigeration power to input PV power at the warm end) was used to compare the performance of different geometries at different frequencies.

Geometries Investigated

The baseline regenerator geometry is that of stainless steel screen with the cold end at 80 K and the warm end at 300 K. The average pressure was 2.5 MPa with a pressure ratio of 1.3. The pressure ratio was kept constant for all the cases investigated here. The frequency of the baseline case was 60 Hz, and the flow at the cold end was made to lag the pressure by 30°. Such conditions are typical of current regenerators. Table 1 lists the various regenerators investigated in this study. All were made of stainless steel and used a conductivity factor (ratio of effective conductivity to that of solid rod) of 0.13, except for case F, where the factor

TABLE 1. Regenerators investigated.

Case	Matrix	f (Hz)	P_0 (MPa)	n_g	Comments
A1	Screen	60	2.5	0.686	Baseline case
A2	Screen	400	2.5	0.686	Same geometry as 1A
A3	Screen	400	7.0	0.686	Same geometry as 1A
B	Screen	400	7.0	0.686	Optimized geometry
C	Screen	1000	7.0	0.686	Optimized geometry
D	Parallel tubes	400	7.0	0.50	Optimized geometry
E	Parallel tubes	1000	7.0	0.50	Optimized geometry
F	Parallel tubes	400	7.0	0.60	f_{cond} = 1.0, opt. geometry

was 1.0. The factor accounts for the presence of many boundaries between each screen layer. The factor of 0.13 was based on previous measurement of thermal conduction of stacked stainless steel screen [6]. The baseline case is A1 in Table 1. Several runs of REGEN3.2 were made to find the geometry that gave the maximum coefficient of performance *COP*. Then the *COP* of the same geometry was calculated when the frequency was increased to 400 Hz. That is designated case A2. Next the pressure was increased to 7.0 MPa with no change to the geometry. That is designated case A3. Case B is for the screen at 400 Hz and 7.0 MPa, but with the geometry optimized. Case C is for screen optimized at 1000 Hz and 7.0 MPa. Case D, E, and F are for parallel tubes (holes) in a stainless steel matrix. For these cases no external tube is required to contain the pressure. The conductivity factor of 0.13 was used in case D and E, but case F had a factor of 1.0 to show the effect of the increased conduction. Theoretically, tubes give better regenerator performance because of the higher value of α in equation (9).

Numerical Results

For each case given in Table 1 the length, hydraulic diameter, and gas cross-sectional area per unit mass flow at the cold end were varied to find the maximum *COP*. Porosity could have been varied, but we chose not to do any detailed studies with that variable. Table 2 gives

TABLE 2. Results of regenerator optimization.

Case	Matrix	f (Hz)	P_0 (MPa)	$A_g / \dot{m}$ (cm^2-s/g)	L (mm)	D_h (μm)	ϕ_c (deg.)	ϕ_h (deg.)	P_{rh}	*COP*
A1	Screen	60	2.5	0.640	45	55.4	-30	29	1.36	0.127
A2	Screen	400	2.5	0.640	45	55.4	-30	76	1.60	0.0060
A3	Screen	400	7.0	0.640	45	55.4	-30	83	1.36	-0.0161
B	Screen	400	7.0	0.146	12.0	16.0	-30	32	1.41	0.0993
C	Screen	1000	7.0	0.0965	7.0	12.0	-40	25	1.45	0.0863
D	Tubes	400	7.0	0.135	11.0	10.0	-30	24	1.37	0.130
E	Tubes	1000	7.0	0.106	6.0	7.0	-40	22	1.39	0.120
F	Tubes k_{cond} =1	400	7.0	0.109	18.0	14.0	-30	36	1.38	0.0952

the results of the numerical analyses with REGEN3.2 on the optimized geometry for all of the cases. The baseline 60 Hz case has *COP* = 0.127. As expected, it has a nearly linear temperature profile as shown in Figure 2. If the frequency is increased to 400 Hz in the same regenerator (case A2), nearly all of the net refrigeration is lost. The *COP* is only 0.0060 for that case. The high frequency in the relatively large gas volume causes the vertical phasor in Figure 1 to become very large, which leads to a large phase angle at the warm end (ϕ_h = 76°) and a large flow rate at that end. The losses associated with the large mass flow are large enough to nearly eliminate any net refrigeration power at this high frequency. The large phase angle causes the temperature profile in this case to be skewed upward very significantly, as shown in Figure 3. If any measured temperature profile has this shape, it is a good indication that the flow is leading the pressure by much more than that required for optimum behavior.

Increasing the pressure to 7.0 MPa with no change in the geometry makes the problem even worse, as indicated by the negative *COP* for case A3. However, when the regenerator volume is significantly reduced in an optimized way (case B), the flow phase at the warm end is reduced to 32°, only slightly higher than the 29° phase of the 60 Hz case. The *COP* of 0.0993 is 78 % of that of the 60 Hz case. The required hydraulic diameter of 16 μm may be difficult to obtain in stainless steel screen, but the result here provides guidance to experimental requirements. Increasing the frequency to 1000 Hz with some reduction in the regenerator volume yields a *COP* for case C of 0.0863, or about 68 % of that of the 60 Hz case. With the optimization described here the local fluid behavior is nearly the same as that for the baseline case of 60 Hz. For example, the maximum velocity changes from 4.1 m/s to 8.1 m/s. The peak Reynolds number changes from 100 to 120 and the relative penetration at the cold end changes from 0.14 to 0.13. The higher frequency operation does lead to a reduction in the heat capacity ratio between the matrix and the gas flowing through the matrix. For case A1 at 60 Hz the ratio is 164, but for case A3 at 1000 Hz the ratio is reduced to 81. Figure 4 shows how the *COP* of the baseline case varies when the heat capacity of the matrix is artificially varied. As that figure shows, a heat capacity ratio below about 50 causes the *COP* to drop significantly. The higher pressures needed for satisfactory high frequency operation lead to the lower heat capacity ratios. The matrix specific heat is sufficiently high at 80 K that the heat capacity ratio remains above 50 even for operation at 1000 Hz and 7.0 MPa.

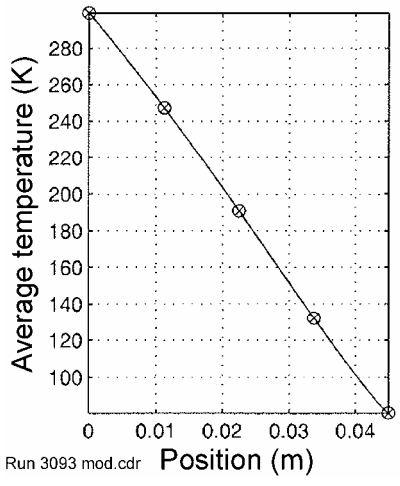

FIGURE 2. Average temperature profile of regenerator for case A1.

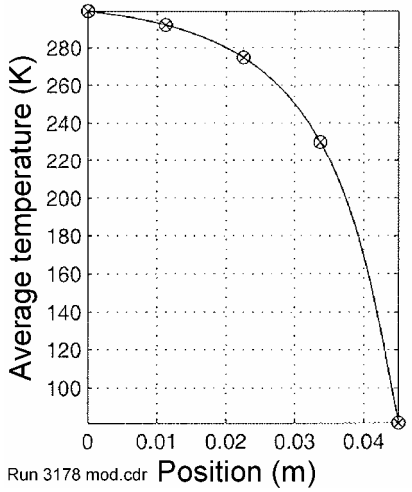

FIGURE 3. Average temperature profile of regenerator for case A2.

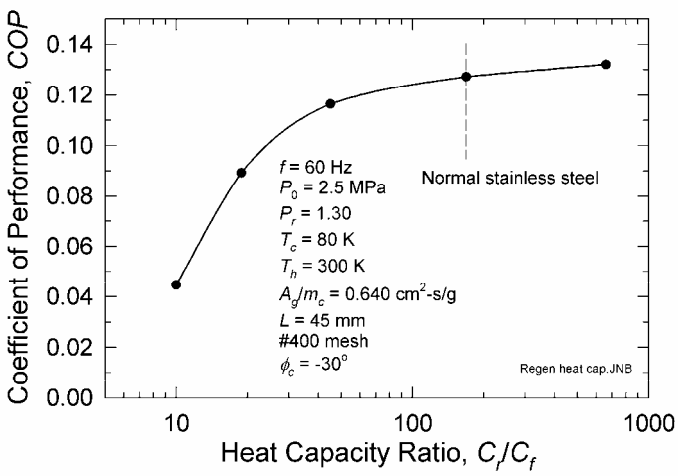

FIGURE 4. Effect on the *COP* of heat capacity ratio between matrix and gas passing through.

However, with temperatures somewhat less than 80 K the lower matrix specific heat will give rise to heat capacity ratios less than 50 at higher pressures and frequencies and contribute to lower values of *COP* at the higher frequencies. Thus, the maximum frequency for reasonably efficient regenerator performance is reduced at lower temperatures. At 4 K it is difficult to maintain good efficiency even at 30 Hz.

Parallel tubes (or holes) have a larger α and yield a smaller volume and a somewhat higher *COP*, as indicated in Table 2. At 400 Hz the *COP* is about the same as that for screen at 60 Hz. At 1000 Hz the *COP* is reduced only slightly compared with that for the 400 Hz case. When the conductivity factor is set to 1.0 (case F) the *COP* at 400 Hz is reduced to 0.0952, although a higher porosity of 0.6 was used for that case to help reduce the conduction loss. Figure 5 summarizes the variation of *COP* for the various cases in a graphical manner.

THERMAL PENETRATION DEPTHS

The thermal penetration depth for oscillating heat transfer is given by

$$\delta_t = \sqrt{(2k / \omega \rho c_p)}, \tag{14}$$

where c_p is the specific heat of the material. As frequency increases the thermal penetration depth decreases. For good heat transfer in the regenerator we require $D_h << 2\delta_t$. Therefore, it is useful to make this comparison for the very high frequency operation of regenerators. Figure 6 shows the temperature and frequency dependence of the thermal penetration depth in stainless steel and in helium gas at two pressures. The smallest thermal penetration depths occur in helium at low temperatures. For helium at 80 K and 2.5 MPa we have for the baseline case A1 at 60 Hz, $2\delta_t/D_h = 2.5$. For case B at 400 Hz and 7.0 MPa we have $2\delta_t/D_h = 3.3$, and for case C at 1000 Hz and 7.0 MPa we have $2\delta_t/D_h = 2.8$. For the tube geometry the ratios are 5.3 for case D, 4.8 for case E and 3.8 for case F. In all cases the ratio is larger than for the baseline 60 Hz case, which indicates the analyses performed here with REGEN3.2 should be valid. The thermal penetration depth in helium at 7 MPa and 1000 Hz is 6.7 times smaller than that at 60 Hz and 2.5 MPa. Thus, pulse tubes of much smaller diameter can be used at the higher frequency and still experience adiabatic processes necessary for high efficiency.

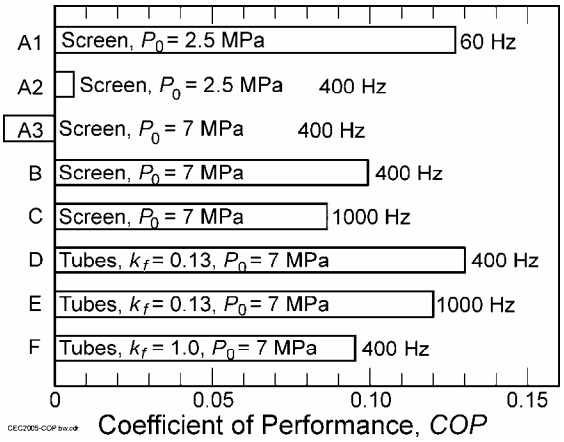

FIGURE 5. Summary of optimized *COP* for various cases.

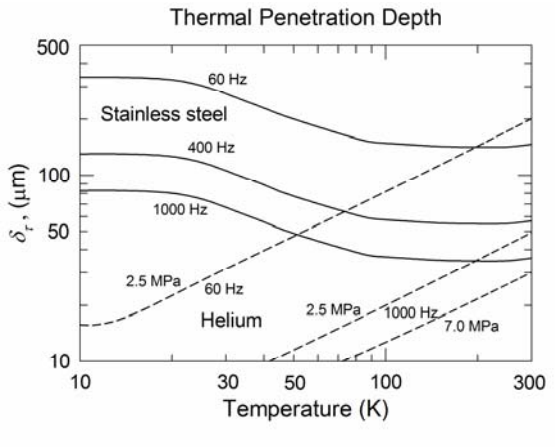

FIGURE 6. Thermal penetration depth of stainless steel and helium.

LINEAR COMPRESSOR SCALING LAWS

For a moving-coil linear motor the volume of the magnet and the back iron are proportional to the volume of the moving coil. For a given PV power the moving-coil volume is given by [7]

$$V_{coil} = \frac{2\rho \dot{W}_{PV}}{\pi^2 p B^2 f^2 s^2 (\dot{Q}_j / \dot{W}_{PV}) \cos^2 \psi}, \tag{15}$$

where ρ is the coil resistivity, p is the coil packing fraction, B is the magnetic field in the gap, f is frequency, s is the piston stroke, $(\dot{Q}_j / \dot{W}_{PV})$ is the ratio of Joule heating to the PV power, and ψ is the phase angle between the motor force and the velocity (ψ = 0 for resonance). From equation (15) we see that for a given PV power the coil volume, and hence the compressor volume, will scale as $1/f^2 s^2$. In order to operate at resonance the inertial force on the moving component must be balanced by the sum of the mechanical spring force and the real part of the gas spring as given by [7]

$$2\pi^2 f^2 sm = \tfrac{1}{2} k_s s + P_1 (\pi d^2 / 4) \cos\varphi, \tag{16}$$

where s is the peak-to-peak stroke, m is the mass of the moving component, k_s is the mechanical spring constant, d is the piston diameter, and φ is the phase between the pressure and the piston motion. For small void volume between the regenerator warm end and the piston we have the approximate relationship

$$\varphi \approx (\pi / 2) - \phi_h. \tag{17}$$

Typically φ is about 30° to 40° for most cryocoolers. Two possible scaling laws that satisfy equation (16) are as follows: (a) for small k_s, $s \propto 1/f^{1/2}$, $d \propto 1/f^{1/2}$, $m \propto 1/f^{5/2}$; (b) for large k_s, $s \propto 1/f^{1/2}$, $d \propto 1/f^{1/2}$, $m \propto 1/f^2$. Case (a) would require significant effort to lighten the mass at high frequencies (hollow components) whereas case (b) would be slightly easier to achieve. The stiff springs in case (b) are also desirable for centering the piston. In both cases

the swept volume would scale as $V_{co} \propto 1/f^{3/2}$. That would require the scaling of P_0 according to equation (5) to be $P_0 \propto f^{1/2}$. In both cases equation (15) then shows that the coil volume, and probably the compressor volume, would scale as $V_{coil} \propto 1/f$. The fact that the moving mass scales at least as fast as $1/f^2$ means that at some high frequency the mass will be dominated by that of the coil, and any further decrease in size with frequency will not be possible. The scaling discussed here shows that by increasing the frequency from 60 Hz to 600 Hz the compressor volume and mass can potentially be reduced by an order of magnitude.

CONCLUSIONS

Analytical equations were developed here that showed that regenerators could be operated at frequencies up to about 1000 Hz without large increases in the losses, provided that the average pressure was also increased up to about 7 MPa. The NIST numerical model REGEN3.2 was used to optimize the geometry of screens and parallel tubes for use at frequencies up to 1000 Hz for a cold-end temperature of 80 K and a warm-end temperature of 300 K. For screen geometry the coefficient of performance at 400 Hz for the optimized geometry was about 78 % of that at 60 Hz. For 1000 Hz the ratio dropped to 68 %. Parallel tubes yielded calculated values for *COP* at 400 and 1000 Hz about the same as that at 60 Hz for screen. Much smaller hydraulic diameters and smaller regenerator volumes are required for the very high frequency operation at high pressures. The scaling laws proposed here show that as the operating frequency is increased from 60 to 600 Hz the volume and mass of the compressor could be reduced by about an order of magnitude for nearly the same refrigeration power. Such size reductions are particularly important for space applications and for the development of microcryocoolers for MEMS applications.

REFERENCES

1. Radebaugh, R., Lewis, M., Luo, E., Pfotenhauer, J. M., Nellis, G. F., and Schunk, L. A., "Inertance Tube Optimization for Pulse Tube Refrigerators," in *Advances in Cryogenic Engineering*, vol. 51, American Institute of Physics, 2006 (This publication) (to be published).
2. Radebaugh, R., and Louie, B., "A Simple, First Step to the Optimization of Regenerator Geometry," in Proc. 3rd Cryocooler Conference, NBS Special Publication 698 (1985), pp. 177-198.
3. Radebaugh, R., "Microscale Heat Transfer at Low Temperatures," in *Microscale Heat Transfer – Fundamentals and Applications*, S. Kakac, *et al.* (eds.), Springer, the Netherlands, 2005, pp. 93-124.
4. Gary, J., Daney, D. E., and Radebaugh, R., "A Computational Model for a Regenerator," in *Proc. Third Cryocooler Conf., NIST Special Publication 698* (1985), pp. 199-211.
5. Gary, J. and Radebaugh, R., "An Improved Model for the Calculation of Regenerator Performance (REGEN3.1)," in *Proc. Fourth Interagency Meeting on Cryocoolers*, David Taylor Research Center Technical Report DTRC91/003 January 1991, pp. 165-176.
6. Lewis, M. A., and Radebaugh, R., "Measurement of Heat Conduction Through Bonded Regenerator Matrix Materials, *Cryocoolers 12*, Plenum Press, New York, 2003, pp. 517-522.
7. Marquardt, E., Radebaugh, R., Kittel, P., "Design Equations and Scaling Laws for Linear Compressors with Flexure Springs," Proc. 7th International Cryocooler Conference, Air Force Report PL-CP-93-1001, 1993, pp. 783-804.